Commensuration and discommensuration in $2H$-$TaSe_2$

Yasumasa Koyama,* Z. P. Zhang, and Hiroshi Sato
School of Materials Engineering, Purdue University, West Lafayette, Indiana 47907
(Received 11 February 1987)

Changes of satellite dark-field images of the incommensurate phase in $2H$-$TaSe_2$ upon cooling are examined closely in order to investigate the behavior of the incommensurate-commensurate transition of this material. Moirélike fringes observed in the higher temperature range of the phase, which were confirmed to be due mostly to the interference of the first- and second-order diffraction beams from the incommensurate structure in our earlier, high-resolution study, are found to change, starting around 92 K, into the domain images of the commensurate structure which are due mostly to a dark-field diffraction contrast. The change from "interference fringes" to "diffraction contrast" is associated with the change of the modulation mode of the incommensurate phase from the "incommensurate modulation of the normal structure" in the upper temperature range to the "incommensurate modulation of the commensurate structure." The upper temperature range above this transition corresponds to the hexagonal, triply incommensurate state while the lower temperature region is the transition region to the commensurate state. This is in variance with the double honeycomb discommensuration model (a model based on the incommensurate modulation of the commensurate structure) proposed for the explanation of the whole temperature range of the incommensurate phase. The shrinking motion of "jellyfish" patterns (which were called stripples, by Fung *et al.* [J. Phys. C. **14**, 5417 (1981)], or charge-density-wave dislocations by Chen *et al.* [Phys. Rev. Lett. **47**, 723 (1981); Phys. Rev. B **26**, 184 (1982)] for those in $2H$-$TaSe_2$, but "jellyfish patterns" will be used to include these for more general cases and similar ones in other materials), consisting of three discommensuration lines that join at one point in the matrix of the commensurate structure in the transition region, leaves the commensurate structure in its wake and represents the kinetics of the commensuration process. This change in the modulation mode in the incommensurate phase also explains the change of the incommensurability, δ, with temperature in two steps as observed by x-ray diffraction experiments. A theoretical support of this behavior is given.

INTRODUCTION

The material $2H$-$TaSe_2$ is known to exhibit a rich diversity of charge-density-wave (CDW) superlattice phenomena including transitions between fully commensurate, incommensurate, and normal structures,[1] and has thus attracted a large number of both theoretical and experimental investigations especially with respect to the features of the incommensurate-commensurate transition.[2–11] Among these studies, detailed features of the incommensurate-commensurate transition have been made by transmission-electron microscopy by Fung *et al.*[12] and Chen *et al.*,[13] and later by Onozuka *et al.*[14] with high resolution in the temperature range of triply incommensurate phase. The observations of Onozuka *et al.*, however, revealed some incompatible evidence with respect to the interpretation of the triply incommensurate phase. The present work is, therefore, intended to clarify these discrepancies.

The structure of $2H$-$TaSe_2$ is hexagonal with the c axis perpendicular to the metallic layers. The normal to incommensurate and the incommensurate to commensurate transitions occur at ~ 122 and at ~ 83 K, respectively. The symmetry of the structure in the commensurate phase was investigated by convergent-beam electron diffraction and was confirmed to be orthorhombic.[12] This means that, in the commensurate phase region, the homogeneous incommensurate phase should be separated into three distinct domains and these domains can be distinguished by dark-field diffraction contrast.[12,13] Further, satellite dark-field images of the "incommensurate phase" near the incommensurate-commensurate transition temperature revealed that, on heating in particular (the stripe phase), the microstructure was finely separated by stripe domains of other orientations (three kinds of domains are in twin relations[12,13]). Because there is a phase shift of $2\pi/3$ across a domain of other types, this finely separated domain structure corresponds to a discommensurate structure in three directions. Based on this observation, the double-honeycomb discommensuration model was proposed for the explanation of the triply incommensurate phase which has a hexagonal symmetry.[12]

On the other hand, Onozuka *et al.* investigated the high-temperature range of the triply incommensurate phase (specimen temperature ~ 95 K and above) by high-resolution electron microscopy.[14] It was confirmed that the contrast of the satellite dark-field image, which was similar to the moiré pattern, could be explained as being due to the interference of the first- and second-order diffraction beams from the incommensurate structure, and no sign of the existence of domains could be confirmed within the experimental accuracy.[14] A periodic modulation of the CDW lattice image suggested the existence of discommensuration (phase-slip region). However, this could also be explained purely as a result of the interference and could not be identified experimentally as discommensuration.[14] At least, it could be concluded that the incommensurate phase did not have the discommensurate

structure composed of domains of the commensurate structure down to ~95 K. Based on these results, it was suggested that the triply incommensurate phase was intrinsically incommensurate and that the double honeycomb discommensuration model was not appropriate to the explanation of triply incommensurate phase.[14] The experiment, however, could not be extended reliably much below 90 K (the temperature of the stage) because of the limitation of the stage. Therefore, the major thrust of the present work is directed toward elucidating the features of microstructural changes which take place in the incommensurate phase below 95 K in order to find a possible clue for the discrepancies of the work of Onozuka *et al.*[14] with the observations of Fung *et al.*[12] and Chen *et al.*[13] The investigation of the incommensurability δ by x ray shows that δ approaches zero (commensuration) in two steps with temperature[8] as against the monotonic change of δ suggested by the discommensuration theory.[3,6,7,9] The existence of the second step in the δ-T curve, therefore, suggests a change of the modulation mode at around 95 K.

In this paper, we first explore the evidence of the change of the modulation mode from the intrinsically incommensurate phase as observed by Onozuka *et al.*[14] to the modulation by means of domains of the commensurate structure as confirmed by Fung *et al.*[12] and Chen *et al.*[13] Based on the results obtained, we examine the discommensuration theory in terms of the Ginzburg-Landau free energy with respect to a two-step change of δ.

EXPERIMENTAL PROCEDURE

The experiment conducted in this study was essentially the same as that by Onozuka *et al.*,[14] but at somewhat lower temperatures. Specimens of $2H$-$TaSe_2$ were from crystals grown earlier by a vapor-transport technique.[14] The same double-tilting, side-entry, low-temperature stage with liquid-nitrogen reservoir for the JEM 200 CX electron microscope (JEOL Ltd., Tokyo) was used. At this time, however, the copper conduction sheets used earlier (Fig. 1 of Ref. 14) were replaced by those of silver. With a liberal use of silver paint for the mounting of specimens on copper grids, this modified stage showed a better behavior than the earlier one in the lower temperature range and a satisfactory image could be obtained at temperatures as low as 78 K, although the time span during which the temperature drift could be suppressed decreased at lower temperatures. The temperature indicated in this paper is that of the stage as before, and the difference in temperature between the sample and the stage could amount to 5°–7° as in the earlier experiment.[14] Based on the comparison of results with those in the earlier experiments, however, it seems that the difference in temperature between the specimens and the stage is somewhat less in the improved stage.

In order to avoid mechanical vibrations from the bubbling of the coolant, liquid nitrogen was removed from the reservoir immediately before recording images. Because of the large heat capacity of the holder, several pictures could be taken before thermal drift of the specimen became appreciable. The attainable temperature was determined by adjusting the number of silver conduction sheets (and the degree of tightening them) used for controlling the conduction path and by evacuating the liquid nitrogen tank. Because of this situation, experiments at different temperatures are essentially independent experiments. Because of the possible existence of the hysteresis at the commensurate-incommensurate transition point as indicated in earlier experiments,[12,13] special caution was taken not to lower the temperature of the specimen below the incommensurate-commensurate transition temperature when the microstructure of the incommensurate phase was investigated.

RESULTS

In order to facilitate the following discussion, we first show in Fig. 1 a diffraction pattern taken in the incommensurate phase and its schematic representation along one of the major axes. The superlattice spots appear in the directions of the major axes and occupy positions close to the $\frac{1}{3}$ position between two fundamental spots. The deviation of the first order diffraction spot from the $\frac{1}{3}$

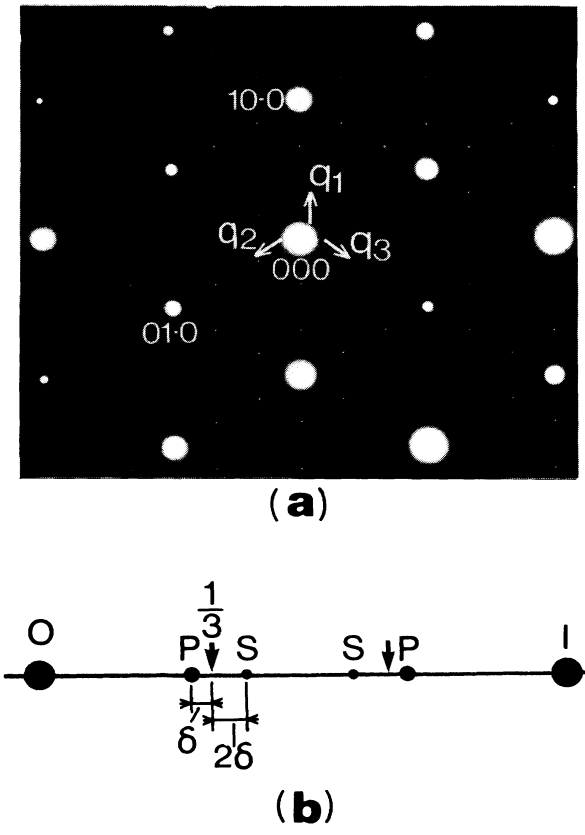

FIG. 1. (a) Electron diffraction pattern in the basal plane of $2H$-$TaSe_2$ at 97 K. The direction of the beam is parallel to the [00·1] direction (Ref. 14). (b) Schematic representation of the diffraction pattern in one of the $[h0{\cdot}0]^*$ direction (Ref. 14). The symbols 0 and 1 represent two fundamental diffraction spots and P and S represent the primary and secondary superlattice diffraction spots respectively. The separation of P and S here is highly exaggerated.

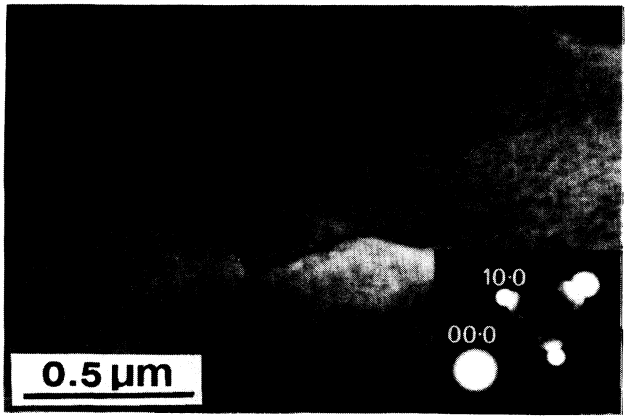

FIG. 2. Dark-field image taken at 100 K utilizing three superlattice spots in the three diffraction directions in the objective aperture.

position is specified by the incommensurability δ. The superlattice spots are split at least into two on either side of the $\frac{1}{3}$ position and these are 3δ apart. Dark-field images taken by the use of the superlattice spots in this temperature range reveal moirélike fringes with a spacing equal to $1/(3\delta)$. Because the superlattice spots lie essentially on the major axes, the dark-field image utilizing one or several of these superlattice diffraction spots can be specified by the diffraction vectors of the superlattice spots, q_1, q_2, and q_3, as shown in Fig. 1.

Dark-field images of the incommensurate phase taken above 100 K are essentially the same as those obtained by Onozuka *et al.*[14] In order to complement the conclusion obtained earlier that the contrast obtained by the dark-field image in this temperature range is due to the interference of the two split spots (P and S shown in Fig. 1, or the first- and the second-order superlattice diffraction spots), in Fig. 2, a dark-field image taken at 100 K by the superpositions of three superlattice spots in three q directions is shown. If the contrast is due to the diffraction contrast from domains of three different orientations, the superposition in three directions would not create any contrast. On the other hand, if the contrast is due to the interference of two split superlattice spots (of one superlattice spot), no such cancellation of intensities would occur by such superposition. Figure 2 shows clearly the superposition of such interference fringes and in agreement with the earlier conclusion that the contrast which produces the moirélike fringes in this temperature range is due mostly to the interference and not to the diffraction contrast expected from the existence of domains of the commensurate structure.

The change in the dark-field images at the same location with changing temperature taken in the three q directions (triple-q imaging) are shown in Figs. 3 to 6. All the images in Figs. 4 to 6 are arranged in the same orientations as in Fig. 3. It should be emphasized here that it is very important to take dark-field images in the three directions at the same location of the specimen in order to obtain reliable conclusions. It was possible to identify the direction and the location of the image

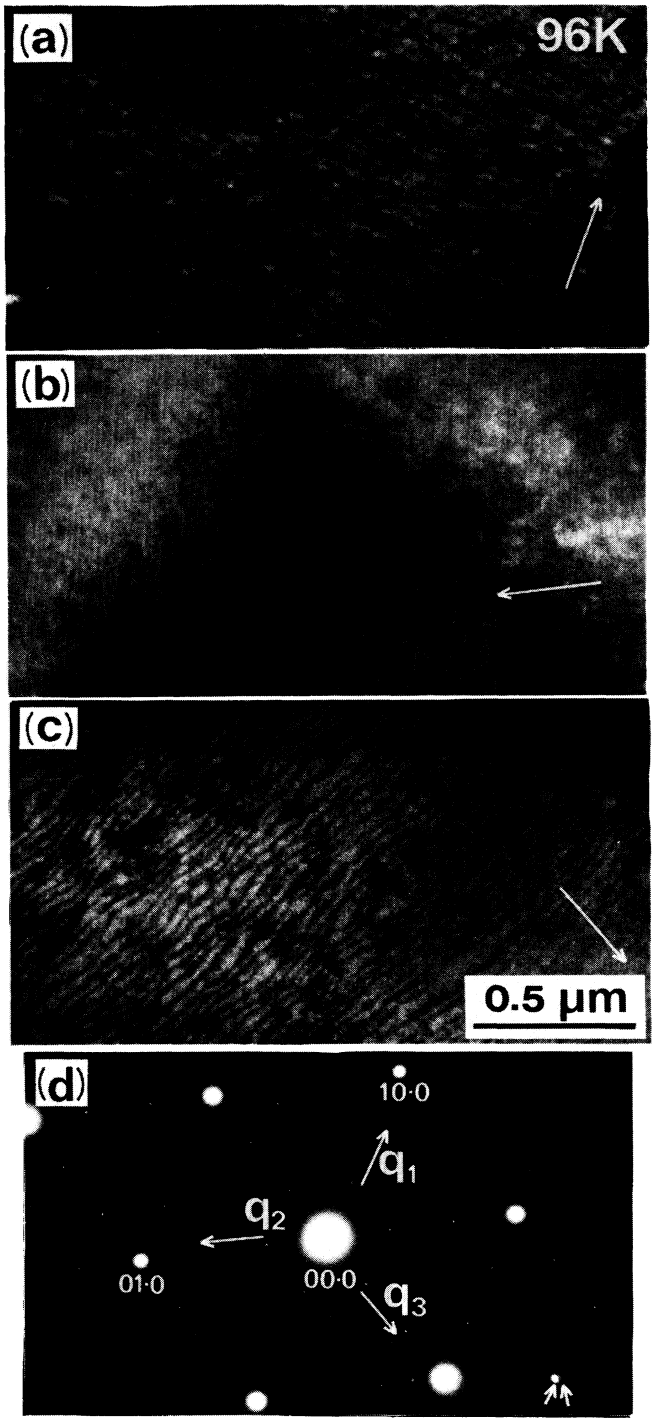

FIG. 3. Satellite dark-field images at 96 K in the triply incommensurate phase for three imaging directions (a) q_1, (b) q_2, (c) q_3, and (d) corresponding electron-diffraction pattern. In (d), three imaging directions are shown by arrows. Inset in (d) shows an enlargement of the pattern near $(\frac{4}{3}\frac{4}{3}\cdot 0)$, indicating split superlattice spots, P and S.

based on the shape of the specimen and, here, the q_2 direction is almost perpendicular to the edge of the specimen. Dark-field images taken at 96 K are shown in Fig. 3. These images are essentially the same as those at 97 K (Fig. 6) in the work by Onozuka *et al.*[14] The spacing of the moirélike fringes is ~ 350 Å. This value agrees well with that calculated from $1/(3\delta)$ (Fig. 8 of Ref. 14), and it seems that the temperature of the specimen is very close to the temperature of the stage. Also, the average orientation of the moirélike fringes is not exactly perpendicular to the imaging direction for the q_1 and the q_3 directions as pointed out by our earlier publication.[14] The normal for the former is rotated somewhat toward the q_3 direction while that for the latter is rotated toward the q_1 direction. Here, some black spots are observed on the moirélike fringes. However, these dark spots can be attributed to some spurious origins such as the radiation damage and the inclusion of other superlattice spots in the objective aperture in taking the dark-field images, etc., and do not seem to have any specific physical meaning based on a number of images taken at the same temperature range.

In Fig. 4, the images taken at 91 K are shown. In the directions of q_1 and q_3, the microstructures still look like moiré fringes but with dark spots which cannot be explained as interference fringes. On the other hand, in the q_2 direction, the dark spots clearly spread into triangular or rhombus-shaped areas as indicated by arrows. At 90 K shown in Fig. 5, these dark spots show a systematic development. The contrast of the image is thus found to change from that of interference at high temperatures into that of dark-field diffraction contrast as seen from the reversal of the contrast by changing the imaging direction. In the q_1 and q_3 directions, not only is the contrast derived from diffraction contrast, but also the moirélike fringes change into stripes (when the con-

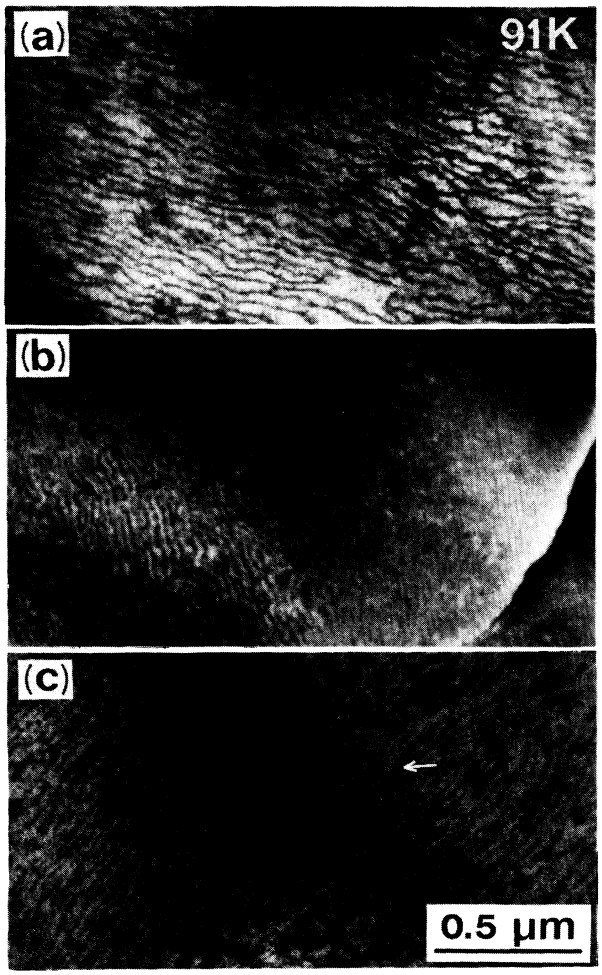

FIG. 4. Dark-field images taken at 91 K in three imaging directions. Dark, spotty (in the q_1 and q_3 directions) and extended (in the q_2 direction) contrasts in the image are indicated by arrows.

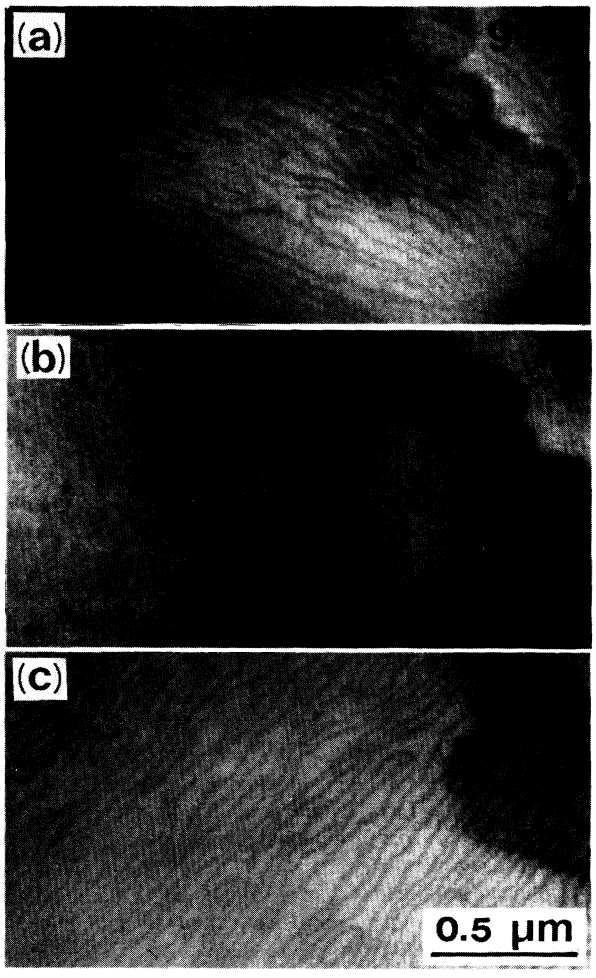

FIG. 5. Dark-field images taken at 90 K in the three imaging directions, showing the development of the dark contrast regions. The formation of JFP's (stripples) is observed in images in the q_1 and the q_3 directions.

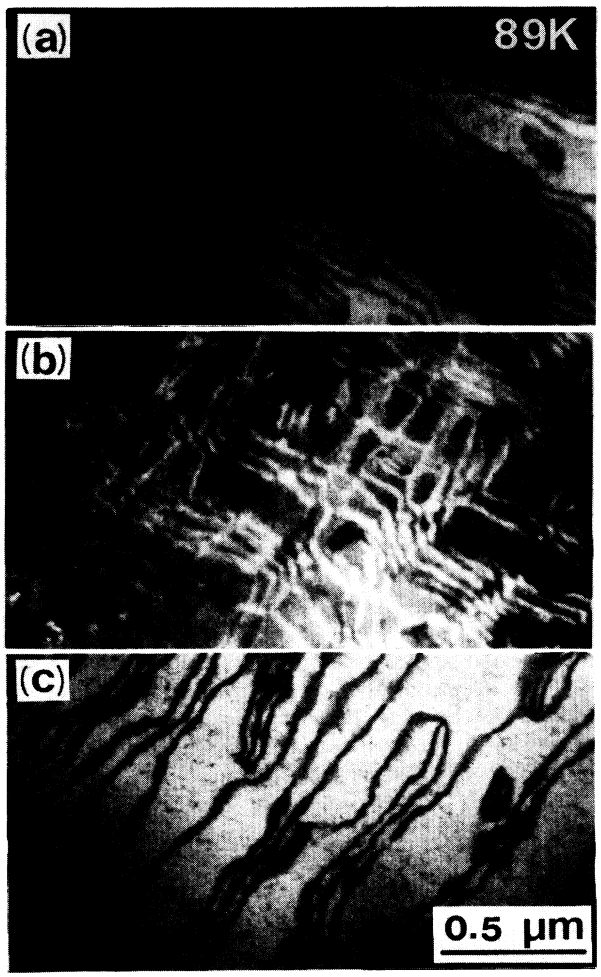

FIG. 6. Dark-field images at 89 K in the three imaging directions, showing the development of dark contrast areas into those of domains.

trast changes into that of diffraction contrast, the fringes are called stripes here) with a large number of stripples as called by Fung *et al.*[12] (or CDW dislocations as called by Chen *et al.*[13]). On the other hand, in the q_2 direction, dark spots now continue to grow into a sizable area of rhombus shape.

The development becomes even clearer in images at 89 K as shown in Fig. 6. In the q_1 and q_3 direction, the number of stripes further decreases and most of them form stripples, indicating that the formation of stripples and their shrinking motion represent the commensuration process which reduces the number of stripes. On the other hand, in the q_2 direction, the dark areas develop into rhombus-shape areas. Also, it is now clearly seen that the black stripe areas in the q_1 and the q_2 directions correspond to white areas in the q_3 direction, and at their intersections, the contrast is missing. Based on these observations of the change in contrast, black regions in the q_1, q_2, and q_3 directions are domains of orthorhombic symmetry with the c-direction parallel to the q_1, q_2, and q_3 directions respectively so that they are mutually in twin relations according to the analysis of Fung *et al.*[12] Features obtained here are thus essentially the same as those obtained in the earlier work[12,13] near the lock-in transition temperature.

The relation between domains in the q_1 and q_3 directions which form stripes was further investigated at 89 K by taking the dark field images shown in Fig. 7. The image in Fig. 7(a) was taken in the q_1 direction, and, that in Fig. 7(b) was taken utilizing two superlattice spots in the q_1 and q_3 directions. This shows that the image 7(b) is the superposition of the stripes in the q_1 and q_3 directions expected from diffraction contrast. Interesting features here are that the heads of stripples always touch the stripes in the other direction. In other words, stripples tend to nucleate or to stop at domain boundaries.

In the present specimen, we have noticed that stripes develop only in the q_1 and q_3 directions and, hence, in the

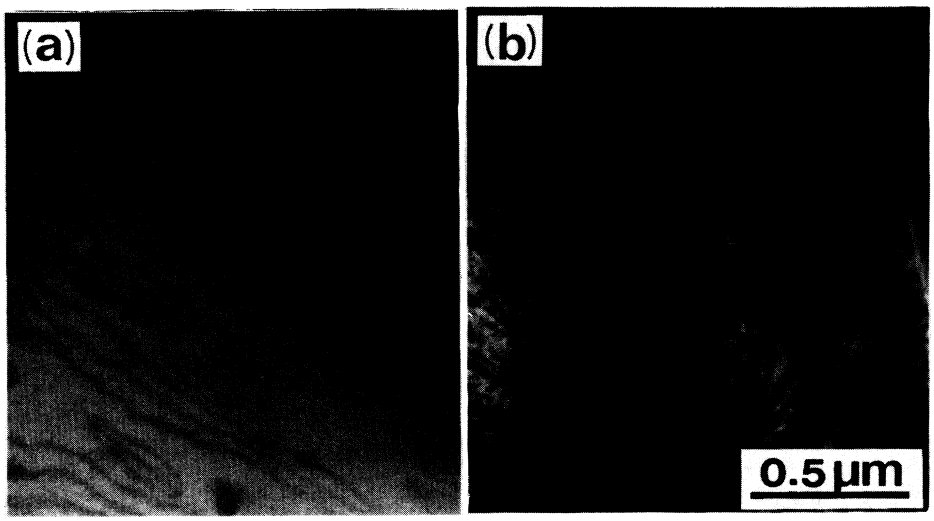

FIG. 7. Dark-field images at 89 K, taken by (a) using superlattice spots in the q_1 direction and by (b) using spots both in the q_1 and the q_3 directions.

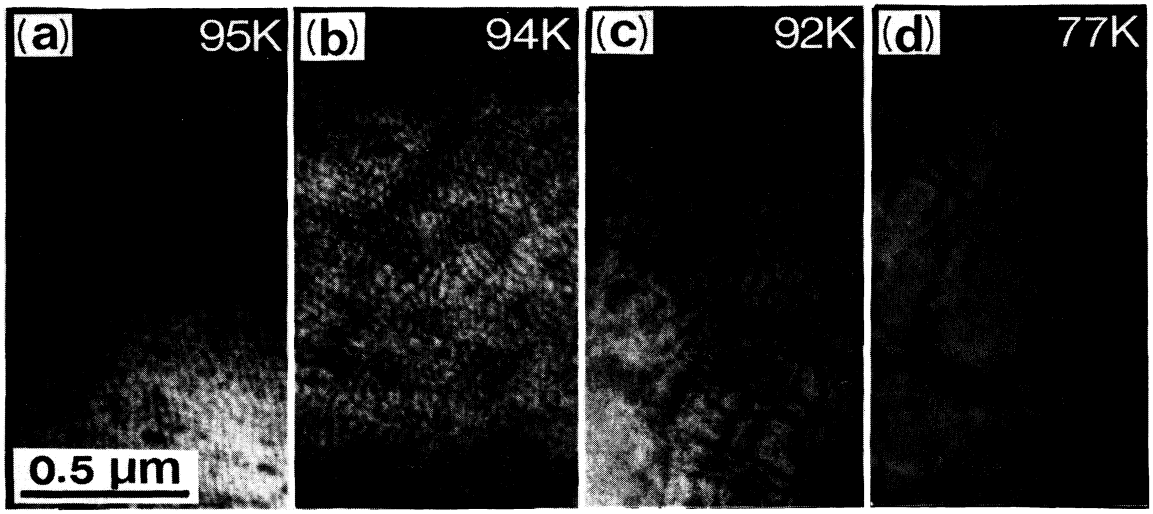

FIG. 8. Dark-field images showing the development of domains in the q_2 direction on lowering temperatures.

q_2 direction, domains of rhombus shape develop. On the other hand, in the earlier work, the stripes were found to develop in the three directions.[12,13] Because of this situation, we show the development of domains in the q_2 direction at a different location of the specimen over a temperature range of 95–78 K in Fig. 8. Except for the change in the contrast (from white to black), the development of q_2 domains is similar to what was observed in Figs. 3–6. The anisotropy in the behavior of development of domains in the q_2 direction in our specimen may be related to internal strain, because the observation was made near the edge of the cleaved specimen and q_2 is perpendicular to the edge. It may be interesting to note here that, at 78 K, the domain structure is yet essentially similar to that observed in the incommensurate state observed at 89 K [Fig. 6(b)]. It seems that, in order for domains in the commensurate state to develop fully, it is necessary to lower the temperature further.[13]

In Fig. 9, dark-field images taken at the same place but at different temperatures indicate the nucleation of stripples. These images were taken at 95 and 94 K, respectively. An interesting feature is that the fringes at 95 K are wavier than those at 94 K. As indicated by arrows, constricted parts in the arrangement of fringes at 95 K change into stripples at 94 K. By lowering the temperature, these places were found to develop into full fledged stripples.

DISCUSSION

The experiment of Onozuka *et al.*[14] on the incommensurate phase of $2H$-$TaSe_2$ in conjunction with the results of Fung *et al.*[12] and Chen *et al.*[13] has indicated that there should be some fundamental changes in the incommensurate structure below around 95 K. Because of this reason, the change of microstructures in the transition region was examined critically. Examinations by means of satellite dark field image revealed that the contrast (of the moirélike fringes) in the high-temperature range could be explained based on the interference of the split superlattice spots (mainly, the first order and the second diffraction spots) from the incommensurate phase as before, but that domains with the structure of orthorhombic symmetry start to develop below around 95 K and spread fast. Below this temperature, the contrast of the dark-field images thus change from that of interference fringes to that of domains due mainly to the diffraction contrast.

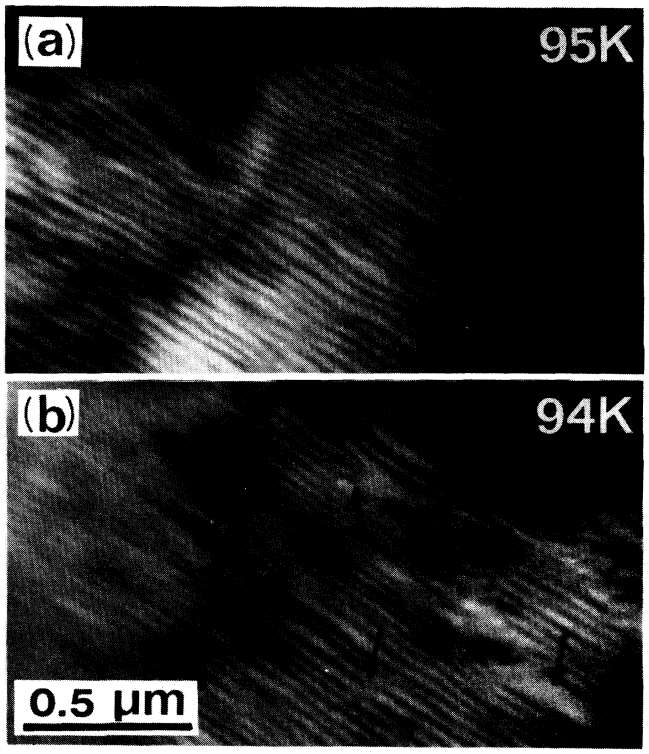

FIG. 9. Dark-field images showing an initial stage of the formation of JFP's at (a) 95 K and (b) 94 K.

The contrast in this temperature regions had been investigated in detail by earlier workers.[12,13]

This change of the origin of contrast indicates a change of the modulation mode in the incommensurate structure between around 91 and 95 K under the present circumstance. The change of contrast from that of domains to that of moirélike fringes can also be explained in terms of the double-honeycomb model[12] as the size of domains becomes smaller. Therefore, the change of modulation mode suggested here cannot simply be concluded from the change of contrast alone unless a careful study of the microstructure in the upper temperature range of the triply incommensurate phase is made.[14] At higher temperatures, the structure is essentially an incommensurate modulation of the normal structure as expected from the CDW formation. Deviation from the sinusoidal modulation creates the second-order diffraction beam and the interference of this second-order diffraction beam with the first-order diffraction beam creates moirélike fringes as discussed in detail in our previous publication.[14] On the other hand, in the lower temperature region, the contrast is explained as being due to the existence of domains of the structure with orthorhombic symmetry in three different orientations. In other words, in this temperature region, the system is yet incommensurate as observed by diffraction method, but the crystal is finely separated into three kinds of domains of the commensurate structure. This situation we call "incommensurate modulation of the commensurate structure" in contrast to the "incommensurate modulation of the normal structure" at higher temperatures. Micrographs in the lower temperature region of the incommensurate phase such as Fig. 6 show that local domain arrangements are far from symmetric and indicate such a domain structure, or incommensurate modulation of the commensurate structure is not truly a periodic modulation of the lattice. In a sense, this is a discommensurate structure by means of domains. The high-temperature region thus represents the triply incommensurate phase, while, in the lower temperature region, a transition state exists. The state with the incommensurate modulation of the commensurate structure is also found in the long period superlattice in alloys such as in the Ag-Mg alloys.[15,16]

There exists a phase slip of $2\pi/3$ across a domain in the direction of the diffraction vector q.[12,13] Therefore, the existence of the line (stripe) of one type of domain serves as the discommensuration line with the phase shift of $2\pi/3$. The shrinking motion of stripples, in which three discommensuration lines terminate at one point, thus leaves the commensurate structure at its wake and represents the commensuration process. In a hexagonal structure like $2H$-$TaSe_2$, the motion of stripples in two directions is required to realize the commensurate structure. Also, it is clear that the change of the modulation mode into the modulation of the commensurate structure is essential to promote the commensuration process by means of stripples.

The relations among domains of three different orientations in the commensurate phase are essentially those of the double-honeycomb discommensuration model.[12] In the temperature region where the incommensurate modulation of the commensurate structure appears, therefore, the double honeycomb discommensuration model can explain the microstructure well. However, it is not appropriate to extend this model to the higher temperature range where the structure is intrinsically incommensurate.

The observation of the periodic change in the CDW lattice spacing in our earlier experiment seems to indicate the existence of the phase slip region at the dark parts of the moirélike fringes.[14] The existence of such periodic change in the spacing of the lattice image, however, could be explained purely on the basis of the interference of the primary and the secondary diffraction beams from the incommensurate structure, and it was not clear whether this phase slip region physically corresponded to the discommensuration.[14] The increase in the intensity of the second-order diffraction spot and the decrease in δ with decreasing temperature were the only linkages to the development of the discommensuration. However, the nucleation of domains on the dark parts of moirélike fringes in the present observation indicates the existence of strain in the phase slip region, and it seems that this supports the concept that the phase slip region observed by transmission electron microscopy[14] is really related to the discommensuration.

Across the phase slip region, there is an overall phase slip of $2\pi/3$ which comes from the fact that the unit cell of the commensurate structure is nearly equal to three times that of the normal structure.[14] Because of this reason, dark parts of the moirélike fringes can form stripples. The physical meaning of the strippelike patterns in this temperature region is, therefore, somewhat different from those in the low-temperature region. Furthermore, we observe topologically similar patterns (but with different origins and different number of discommensuration lines) in different materials and for different origins. Instead of calling each a different name, therefore, we decided to use the more general name jellyfish patterns (JFP) due to their appearance.[14,15] A detailed observation of the change of dark-field images with temperature was also made by Chen *et al.* and the nucleation of domains was suggested.[13] However, here, the temperature at which the moirélike fringes become visible was attributed to the temperature for the nucleation of domains.[13] In other words, the change of the modulation mode at around 92 K where the moirélike fringes change into the image of domains has never been suggested.

The incommensurability δ is known to approach zero (commensurate state) in two steps on cooling as shown by broken lines in Fig. 10.[8] Also, it is known that the δ-T relation shows a hysteresis on cooling and on heating.[8] This suggests that the incommensurate-commensurate transition in $2H$-$TaSe_2$ is a first-order phase transition as confirmed by a specific-heat measurement.[4] The commensuration process by means of JFP motion does not contradict this concept of a first-order phase transition. Therefore, it is feasible to associate the change of the modulation mode which leads to the commensuration process with a two-step change for δ. In fact, the nucleation of domains at $\sim$92 K corresponds to the temperature at

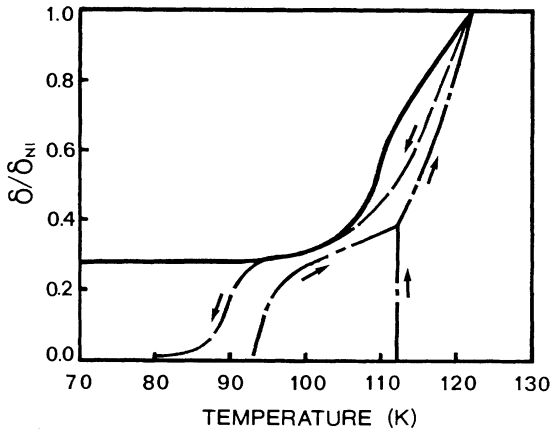

FIG. 10. Comparison of a calculated δ-T curve (solid line) for $N=4$ with experimental one (broken line). The parameters used for the calculation are $b=1.03$, $c=0.139$, and $d=-0.60$. A reduced scale of the incommensurability, δ/δ_{NI}, is used here, where δ and δ_{NI} are the incommensurability at T and at the normal-incommensurate transition temperature T_{NI}, respectively.

which the second step change of δ starts to take place.

Upon heating, the "stripe phase" starts to appear at ~ 92 K and then transforms to hexagonal incommensurate phase at ~ 112 K.[12,13] In this phase, an array of JFP's (or discommensuration lines) grow inside a large domain of the commensurate phase. This is a first order phase transition, and this is the reverse process of the commensuration process in which JFP's recede. The commensuration process occurs in the temperature range 92–83 K while the "discommensuration process" takes place between 92–112 K. The growth of arrays of JFP's in the stripe phase from the commensurate phase is phenomenologically similar to the growth of the long-period superlattice CuAu II from CuAu I (CuAu I and CuAu II are both ordered structures which appear in the stoichiometric region in the Cu-Au alloys, but CuAu I has the normal ordered structure while CuAu II is the long period superlattice[17]) upon heating.[18] Whether the phase such as the stripe phase with the incommensurate modulation of the commensurate structure, however, is really a stable phase or not is not yet clear.

The δ-T relation observed is concave upwards and δ does not reach zero at a finite temperature before the second-step change takes place. On the other hand, the discommensuration theory by McMillan[3] and by Nakanishi *et al.*,[7] indicates that the δ-T curve is convex upward and the incommensurate-commensurate transition is a second order phase transition. Although it is possible to convert the behavior to a first-order phase transition by introducing extra terms such as attractive interaction among discommensuration lines,[9] it is not possible to make the δ-T relation concave. An examination of the discommensuration theory of McMillan[3] and Nakanishi *et al.*,[7] however, reveals that, in order to make δ zero, it is necessary to include a large number of higher harmonics of CDW into the calculation (Appendix). This inclusion, however, makes the δ-T curve convex. On the other hand, based on our observation, although the contribution of the second order harmonic is large, the existence of higher harmonics has not been confirmed. In other words, although the contribution of some higher harmonics should be allowed in order to explain the contrast of moirélike fringes, the amplitude of higher harmonics seems to be extremely small,[14] and, hence, the number of higher harmonics to be included in the discommensuration theory should be limited in the case of $2H$-$TaSe_2$. If the number of higher harmonics, N, is small, it is possible to make the δ-T curve concave and to let δ approach a finite value (see the Appendix). The best fit to the experimental curve can be obtained for $N=4$ and an example is shown in Fig. 10.

By using the same parameter for calculating the δ-T relation, the free-energy curves for the incommensurate and commensurate phases are calculated. For the case of $N=4$, the incommensurate-commensurate transition is found to occur as a first order phase transition in a temperature range where the δ-T relation becomes independent of temperature. In other words, the observation of the change of the modulation mode in the incommensurate phase is consistent with other physical properties of $2H$-$TaSe_2$. A brief explanation of the calculations in terms of the Ginzburg-Landau free energy is given in the Appendix.

ACKNOWLEDGMENTS

Discussions with Professor M. Hirabayashi and Dr. T. Onozuka at the Research Institute for Iron, Steel and Other Metals, Tohoku University, Sendai, Japan, and critical reading of the manuscript and comments by Professors G. L. Liedl and N. Otsuka of School of Materials Engineering, Purdue University are gratefully acknowledged. For the modification of the low temperature stage used in this experiment, we also owe thanks to Dr. T. Taoka of JEOL, Ltd., Tokyo, Japan. The work was supported by the National Science Foundation, Solid State Chemistry Program, Grant No. DMR 8304314, and US-Japan Cooperation Program Grant No. INT84-12550. The international cooperation was possible also by the support of the Japan Society for the Promotion of Science.

APPENDIX: DEVELOPMENT OF DISCOMMENSURATION IN TRIPLY INCOMMENSURATE PHASE (REF. 19)

Here, we deal with the calculation of the change of the incommensurability δ with temperature in the triply incommensurate phase by means of the Ginzburg-Landau-free-energy formalism. Based on the data obtained, it is reasonable to assume that the hexagonal, triply incommensurate state can be treated simply as the superposition of three single states and, hence, we construct the free energy of the single-Q state in a hexagonal layer as originally derived by McMillan.[3] In dealing with the development of higher harmonics with the progress of discommensuration, not only the phase modulation, but also the amplitude modulation is taken into account based on the treatment of Nakanishi *et al.*[6,7]

The free energy F of the system with the charge density wave in one dimension can be expressed as

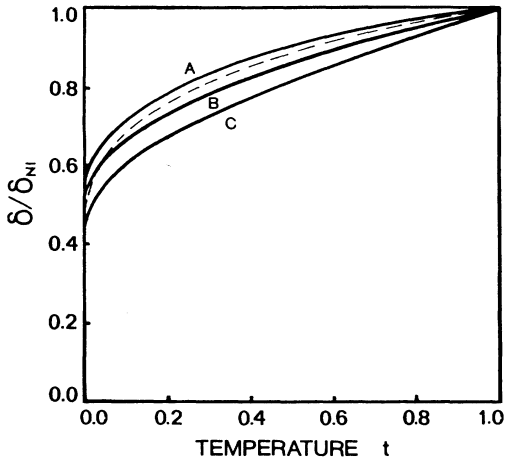

FIG. 11. The change of the δ-T relation with change of the parameter d calculated by Nakanishi *et al.* (Ref. 7) for $N=31$. The parameters used are $b=1.00$; $c=0.069$; and $d=-0.10$ (A), -0.30 (B), and -0.40 (C). The result obtained by McMillan (Ref. 3) is added as a dotted line. A reduced temperature scale $t=(T-T_{IC})/(T_{NI}-T_{IC})$ is used here, where T_{IC} is the incommensurate-commensurate transition temperature.

$$F=\int dx[a(T-T_{NI})\,|\,\eta\,|^2+b\,|\,\eta\,|^4 +c\,|\,(\delta-\delta_{NI})\eta\,|^2+d\,\mathrm{Re}(\eta^3)]\ . \tag{A1}$$

Here, T is the temperature, T_{NI} is the normal to incommensurate transition temperature, δ and δ_{NI} are the incommensurability at T and T_{NI}, respectively. The complex order parameter η is defined in relation to the charge density wave ρ with the wave vector very close to $K/3$ (only δ apart), where K is the reciprocal-lattice vector of the normal state and is expressed as

$$\rho=\mathrm{Re}(e^{i(K/3)x}\eta)\ . \tag{A2}$$

Due to the existence of higher harmonics around $\frac{1}{3},\eta$ in Eq. (A2) can be expressed as[7]

$$\eta=\sum_{m}^{N}\eta_m\exp[i(2m+1)\delta x]\ . \tag{A3}$$

The coefficients a, b, c, and d in Eq. (A1) are taken as adjustable parameters. In the calculation, all these coefficients are normalized with respect to a [which is equivalent to formally taking $a=1$ in Eq. (A1)]. Also, both temperature T and the incommensurability δ are normalized with respect to T_{NI} and δ_{NI}. In this form, the first and the second terms in (A1) are Landau free-energy expression for second-order phase transition. The third term is the so-called elastic term and resists the change of δ from δ_0 determined by the "Fermi-surface nesting" and the fourth term is the umklapp term which tends to make the wave length of CDW commensurate with the normal lattice. Therefore, these two terms compete with each other to determine the temperature dependence of δ. The determination of η_m's is made by minimizing the free energy with respect to η_m's under given T and δ. The value of δ can then be determined for a given T as that which minimizes the free energy.

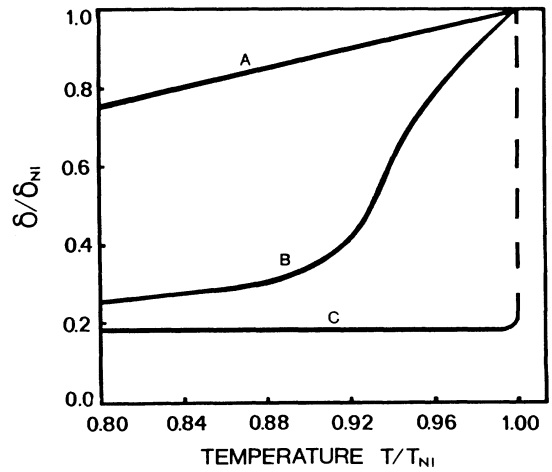

FIG. 12. The change of the δ-T relation calculated for $N=4$ by changing the relative contribution of the elastic term. The parameters used are: $b=1.20$; $d=-0.6$; and $c=0.181$ (A), 0.111 (B), and 0.069 (C).

It has been found that, in order to reach the commensurate state ($\delta=0$), a large number of harmonics [a large N value in Eq. (A3)] are required.[5] Indeed, Nakanishi *et al.* used $N=31$.[7] The comparison of the results of McMillan[3] (which is a phase modulation theory and is equivalent to using $N=\infty$) and those of Nakanishi *et al.*[7] with respect to the δ-T relation for parameters $b=1.00$, $c=0.069$ ($S=1{,}000$), and d which ranges from -0.1 to -0.4 are shown in Fig. 11. (Nakanishi *et al.* used the corresponding parameters B, S, and Y for b, c, and d. Among these, the relations $B=b$, $S=9c/\delta_{NI}^2$, and $Y=d$ exist. Taking the value $\delta_{NI}=0.025$, we obtain the relation $c=0.06944S\times10^{-3}$). The δ-T relation thus

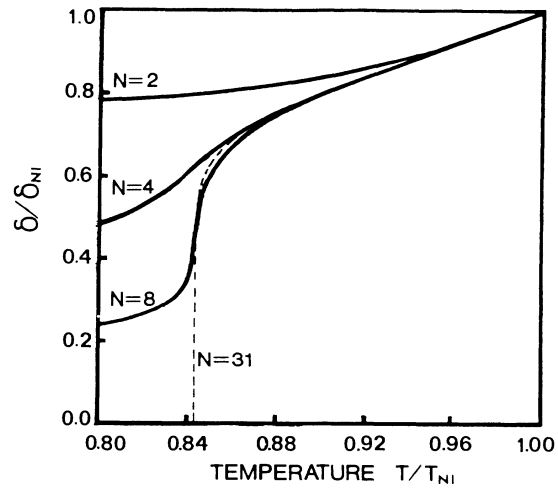

FIG. 13. The change of the δ-T relation with N. The parameters used are $b=1.00$, $c=0.069$, and $d=-0.30$.

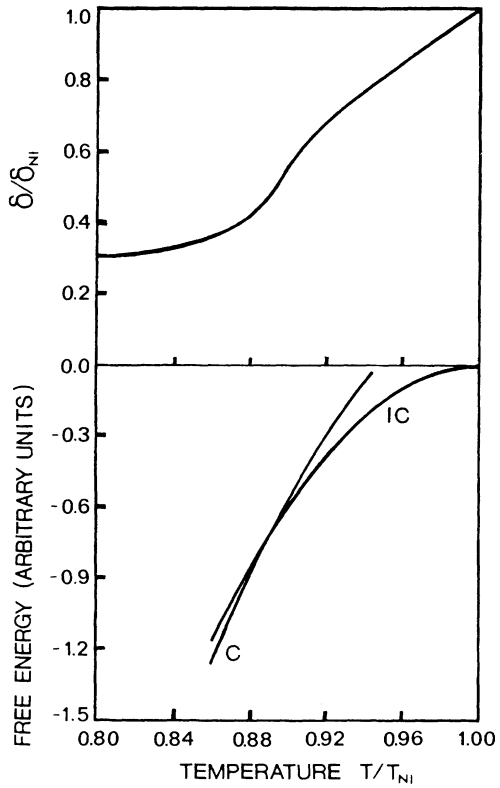

FIG. 14. The temperature dependence of the free-energy curves for the incommensurate state (IC) and the commensurate state for $N=4$. The δ-T relation for the incommensurate state calculated with the same parameters is added. The parameters used are $b=1.03$, $c=0.139$, and $d=-0.60$.

calculated is convex upwards for both treatments and is certainly different from that obtained experimentally which is shown in Fig. 10. In addition, these calculations show that the amplitude of higher harmonics becomes large at low temperatures.[7] In reality, however, only a strong second-order harmonic is observed, and the existence of higher harmonics has not been detected. This fact indicates that the amplitudes of higher harmonics, even if they exist, should be pretty low and that the number of the contribution of higher harmonics should be limited.

By limiting the contribution of the number of higher harmonics, however, it is found that δ does not reach zero, but rather approaches a finite value by lowering the temperature. Further, the δ-T relation can become concave upward. In Fig. 12, the δ-T relation thus obtained for the case of $N=4$ (P,S, the fourth and the fifth harmonics[14]) depending on the magnitude of d (increasing the contribution of umklapp term) is shown. The curves shown are for parameters $b=1.20$, $d=-0.6$, and c which ranges from 0.069 to 0.181. By increasing the relative contribution of the umklapp term (or by decreasing the relative contribution of the elastic term by decreasing the value of c), δ decreases more rapidly with lowering T and at an appropriate value of c, the curve becomes concave and shows a good agreement with the experiment. If the agreement both with the δ-T relation and the temperature dependence of relative intensity of P and S in the neutron diffraction experiment is the goal, the combination of parameters $b=1.03$, $c=0.139$, and $d=-0.60$ gives a better overall agreement. In Fig. 10, the δ-T relation calculated with these parameters is thus plotted and compared with the experiment. The calculation was extended to the case of $N=8$. In Fig. 13, the change of the δ-T relation with N for $N=2$, 4, 8, and 31 with parameters $b=1.00$, $c=0.069$, and $d=-0.30$ is shown in order to show the effect of N. The selection of parameters taken for all of these calculations remain within the same order of magnitude as those taken in the calculation by Nakanishi *et al.*[7] Although no proof could be given that, for large N, the δ-T relation never becomes concave, the results of calculation in Figs. 11–13 show rather convincingly that the contributions of higher harmonics should be limited in accordance with the diffraction data, and that this leads to a qualitative agreement of the δ-T curve with experimental data.[8]

In Fig. 14, the temperature dependence of the free energy for the incommensurate state and for the commensurate state ($\delta=0$) calculated with the same parameters as the δ-T curve for $N=4$ shown in Fig. 10, is plotted. These two free-energy curves are found to intersect in the temperature range where the δ-T curve becomes independent of temperature. The result thus supports our conclusion that the state below the second step of the δ-T curve (and in the stripe phase region upon heating) is the transition region where the commensuration process takes place.

*On leave of absence from Tokyo Institute of Technology, Ohokayama, Meguro-Ku, Tokyo, Japan.

[1]J. A. Wilson, F. J. DiSalvo, and S. Mahajan, Adv. Phys. **24**, 117 (1975).
[2]M. Barmatz, L. R. Testardi, and F. J. DiSalvo, Phys. Rev. B **12**, 4367 (1975).
[3]W. L. McMillan, Phys. Rev. B **12**, 1187 (1975); **14**, 1496 (1976).
[4]R. A. Craven and S. F. Meyer, Phys. Rev. B **16**, 4583 (1977).
[5]D. E. Moncton, J. D. Axe, and F. J. DiSalvo, Phys. Rev. B **16**, 801 (1977).
[6]K. Nakanishi and H. Shiba, J. Phys. Soc. Jpn. **44**, 1465 (1978).
[7]K. Nakanishi and H. Shiba, J. Phys. Soc. Jpn. **45**, 1147 (1978).
[8]R. M. Fleming, D. E. Moncton, D. B. McWhan, and F. J. DiSalvo, Phys. Rev. Lett. **45**, 576 (1980).
[9]A. E. Jacobs and M. B. Walker, Phys. Rev. B **21**, 4132 (1980).
[10]B. H. Suits, S. Couturie, and C. P. Slichter, Phys. Rev. B **23**, 5142 (1981).
[11]R. M. Fleming, D. E. Moncton, J. D. Axe, and G. S. Brown, Phys. Rev. B **30**, 1877 (1984).
[12]K. K. Fung, S. McKernan, J. W. Steed, and J. A. Wilson, J. Phys. C **14**, 5417 (1981).
[13]C. H. Chen, J. M. Gibson, and R. M. Fleming, Phys. Rev. Lett. **47**, 723 (1981); Phys. Rev. B **26**, 184 (1982).
[14]T. Onozuka, N. Otuska, and H. Sato, Phys. Rev. B **34**, 3303

(1986).
[15]Y. Fujino, H. Sato, and N. Otsuka, Mat. Res. Soc. Symp. Proc. **62**, 349 (1986).
[16]Y. Fugino, H. Sato, M. Hirabayashi, E. Aoyagi, and Y. Koyama, Phys. Rev. Lett. **58**, 1012 (1987).
[17]H. Sato and R. S. Toth, Phys. Rev. **124**, 1833 (1961); **127**, 469 (1962).
[18]D. W. Pashley and A. E. B. Presland, J. Inst. Metals **87**, 419 (1958-1959).
[19]Zi-ping Zhang, M. Sci. thesis, Purdue University, 1986 (unpublished).

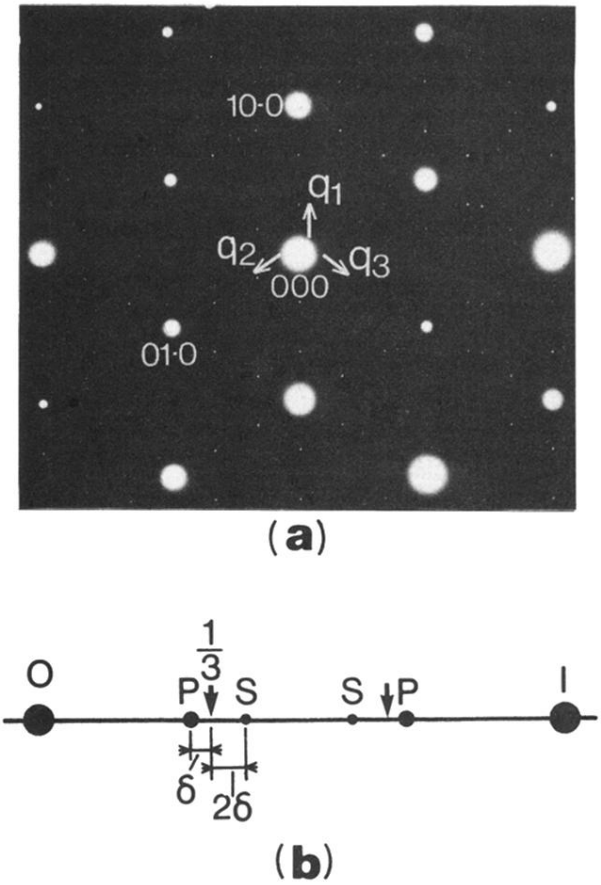

FIG. 1. (a) Electron diffraction pattern in the basal plane of $2H$-$TaSe_2$ at 97 K. The direction of the beam is parallel to the [00·1] direction (Ref. 14). (b) Schematic representation of the diffraction pattern in one of the $[h0{\cdot}0]^*$ direction (Ref. 14). The symbols 0 and 1 represent two fundamental diffraction spots and P and S represent the primary and secondary superlattice diffraction spots respectively. The separation of P and S here is highly exaggerated.

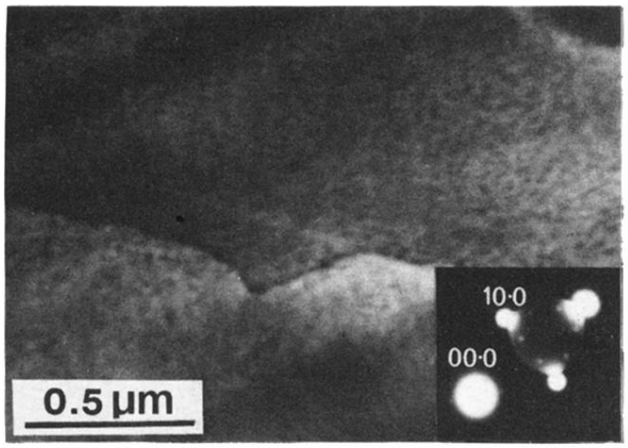

FIG. 2. Dark-field image taken at 100 K utilizing three superlattice spots in the three diffraction directions in the objective aperture.

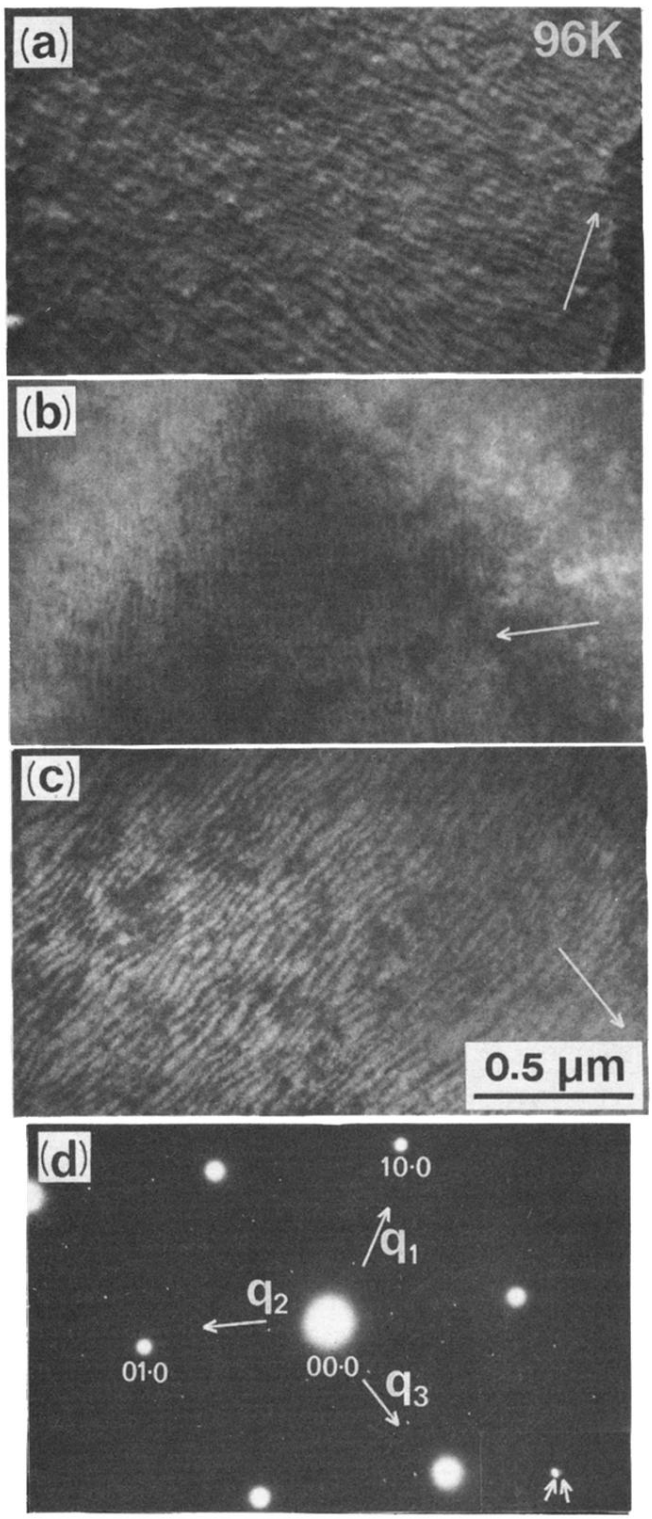

FIG. 3. Satellite dark-field images at 96 K in the triply incommensurate phase for three imaging directions (a) q_1, (b) q_2, (c) q_3, and (d) corresponding electron-diffraction pattern. In (d), three imaging directions are shown by arrows. Inset in (d) shows an enlargement of the pattern near $(\frac{4}{3}\,\frac{4}{3}\cdot 0)$, indicating split superlattice spots, P and S.

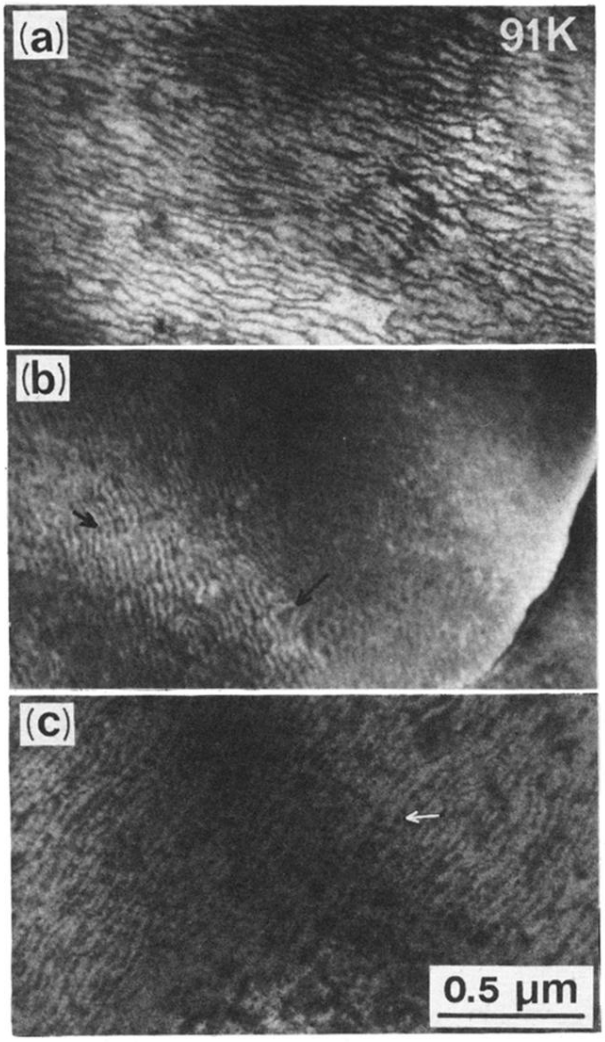

FIG. 4. Dark-field images taken at 91 K in three imaging directions. Dark, spotty (in the q_1 and q_3 directions) and extended (in the q_2 direction) contrasts in the image are indicated by arrows.

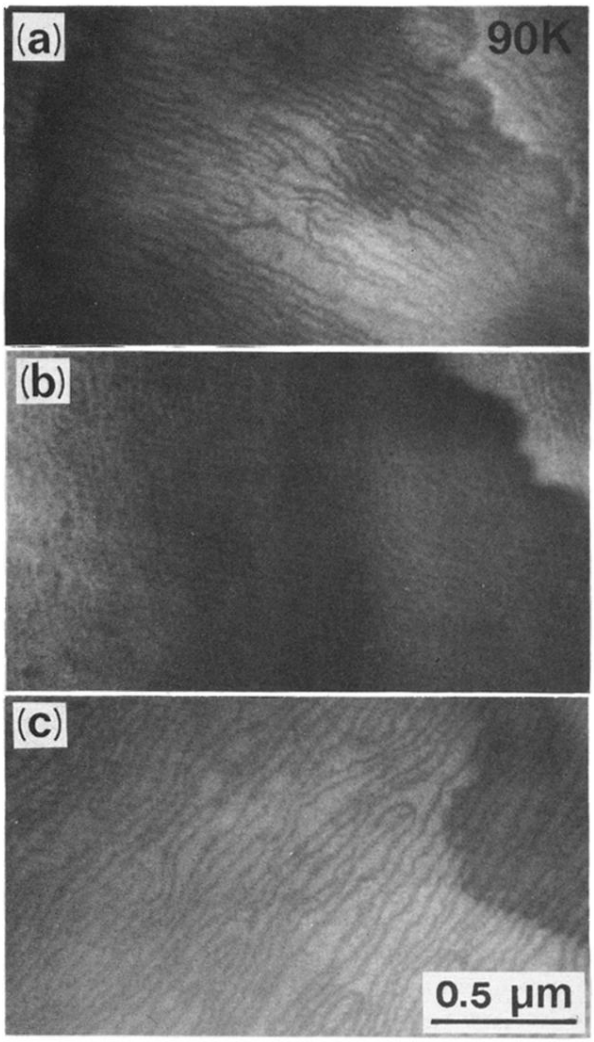

FIG. 5. Dark-field images taken at 90 K in the three imaging directions, showing the development of the dark contrast regions. The formation of JFP's (stripples) is observed in images in the q_1 and the q_3 directions.

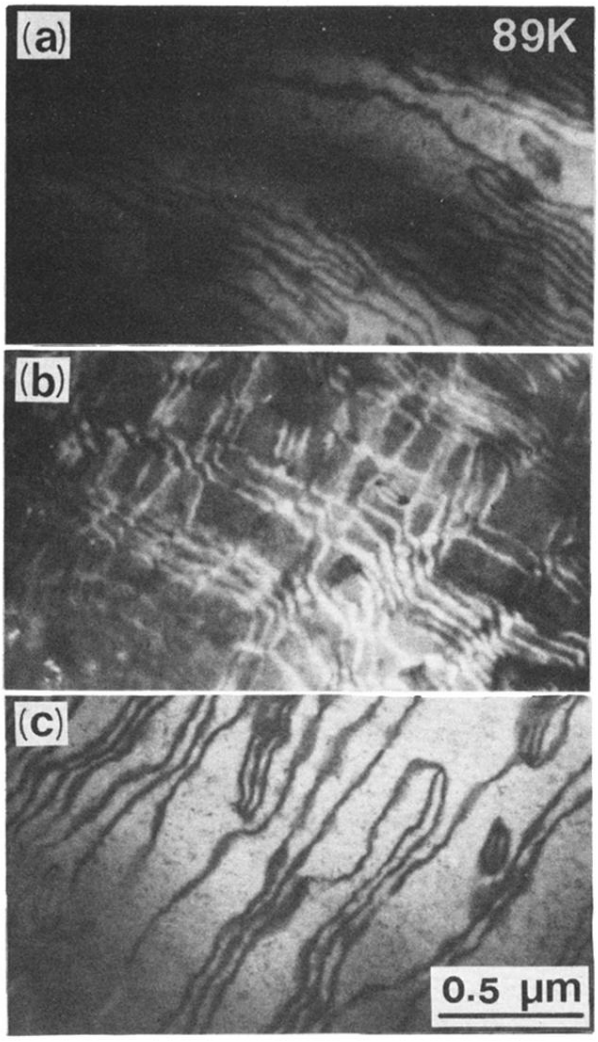

FIG. 6. Dark-field images at 89 K in the three imaging directions, showing the development of dark contrast areas into those of domains.

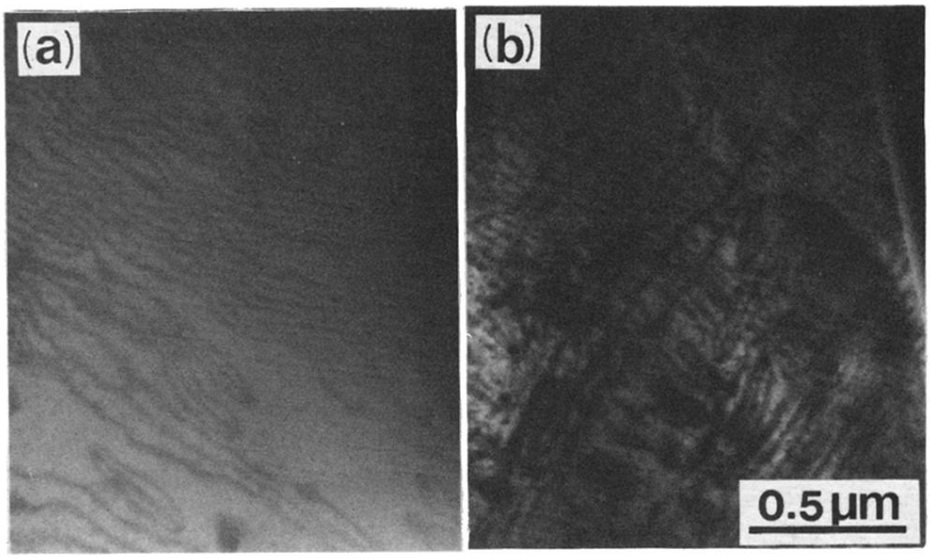

FIG. 7. Dark-field images at 89 K, taken by (a) using superlattice spots in the q_1 direction and by (b) using spots both in the q_1 and the q_3 directions.

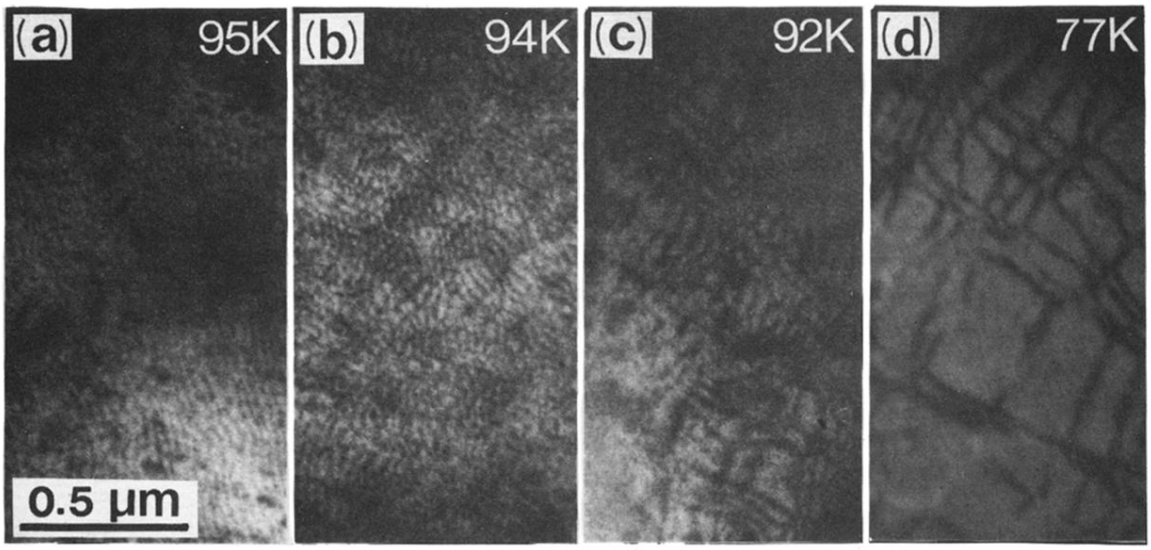

FIG. 8. Dark-field images showing the development of domains in the q_2 direction on lowering temperatures.

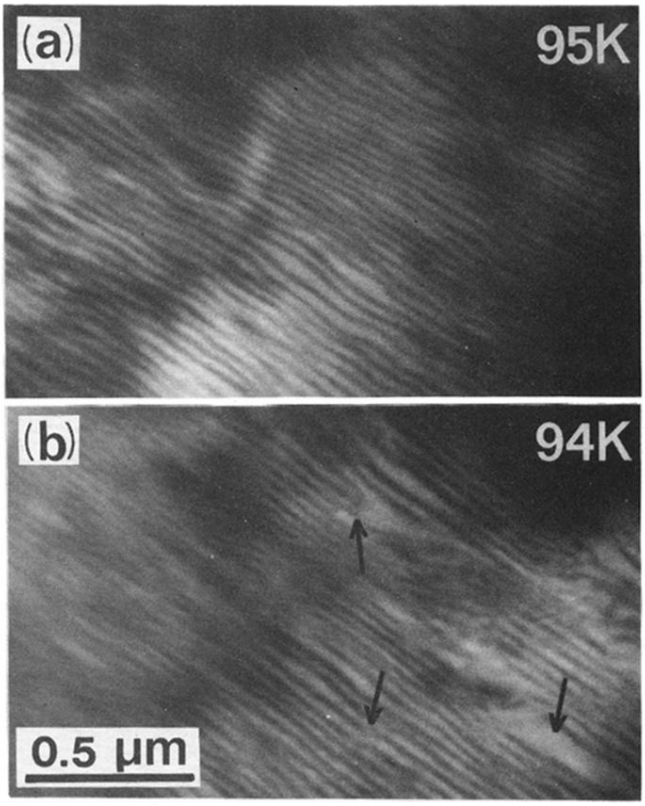

FIG. 9. Dark-field images showing an initial stage of the formation of JFP's at (a) 95 K and (b) 94 K.